ACS APPLIED MATERIALS & INTERFACES

Research Article

www.acsami.org

Airbrushed Nickel Nanoparticles for Large-Area Growth of Vertically Aligned Carbon Nanofibers on Metal (Al, Cu, Ti) Surfaces

Mehmet F. Sarac,[†] Bryan D. Anderson,[†] Ryan C. Pearce,[†] Justin G. Railsback,[†] Adedapo A. Oni,[†] Ryan M. White,[†] Dale K. Hensley,[‡] James M. LeBeau,[†] Anatoli V. Melechko,[†] and Joseph B. Tracy*[,†]

[†]Department of Materials Science and Engineering, North Carolina State University, Raleigh, North Carolina 27695, United States

[‡]Center for Nanophase Materials Sciences, Oak Ridge National Laboratory, Oak Ridge, Tennessee 37831, United States

Supporting Information

ABSTRACT: Vertically aligned carbon nanofibers (VACNFs) were grown by plasma-enhanced chemical vapor deposition (PECVD) using Ni nanoparticle (NP) catalysts that were deposited by airbrushing onto Si, Al, Cu, and Ti substrates. Airbrushing is a simple method for depositing catalyst NPs over large areas that is compatible with roll-to-roll processing. The distribution and morphology of VACNFs are affected by the airbrushing parameters and the composition of the metal foil. Highly concentrated Ni NPs in heptane give more uniform distributions than pentane and hexanes, resulting in more uniform coverage of VACNFs. For VACNF growth on metal foils, Si micropowder was added as a precursor for Si-enriched coatings formed in situ on the VACNFs that impart mechanical rigidity. Interactions between the catalyst NPs and the metal substrates impart control over the VACNF morphology. Growth of carbon nanostructures on Cu is particularly noteworthy because the miscibility of Ni with Cu poses challenges for VACNF growth, and carbon nanostructures anchored to Cu substrates are desired as anode materials for Li-ion batteries and for thermal interface materials.

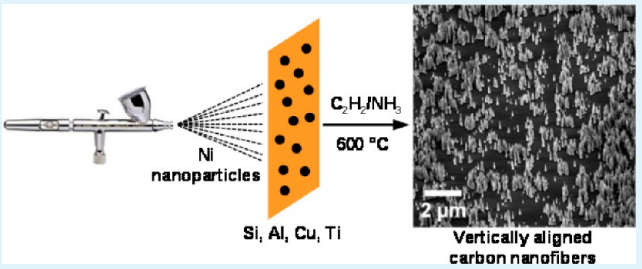

KEYWORDS: *airbrushing, nickel, copper, nanoparticles, catalyst, carbon nanofibers, carbon nanotubes, metal foils*

INTRODUCTION

Vertically aligned carbon nanofibers (VACNFs) have garnered attention for use in diverse applications, including electroanalytical probes,[1−3] gene delivery devices,[4−8] cell-mimetic membranes,[9] neural interfaces,[10−12] sensors,[13−15] electron field-emission sources,[16−20] supercapacitors,[21,22] electrodes for electrocatalysis,[23−26] and batteries.[21] VACNFs are routinely synthesized by catalytic plasma-enhanced chemical vapor deposition (PECVD), which requires the use of catalyst nanoparticles (NPs). Catalytic NPs for VACNF growth are commonly prepared through a combination of traditional photolithography, electron beam lithography, physical vapor deposition, lift-off, and dewetting, which has sufficed for proof-of-principle demonstrations. For example, the arrays used for gene delivery by impaling cells (impalefection) and electron field emission have mostly been produced by high-cost, low-throughput electron beam lithography[27] or slightly less expensive projection lithography.[28,29]

While the use of lithography tools allows for fabrication of precisely defined arrays of VACNFs, such precision is not necessary for some applications. The critical parameters for efficient impalefection and electrodes are the nanofiber aspect ratio and areal density in the array, but periodic ordering among nanofibers is unimportant and comes at significant cost. Catalytic NPs are often prepared by electron beam evaporation or sputter deposition,[29] but such batch processes limit the throughput for manufacturing arrays of VACNFs. Airbrushing of presynthesized catalyst NPs allows for rapid in-air catalyst deposition and still provides a highly monodisperse NP size distribution. Moreover, airbrushing[30,31] is a simple, inexpensive method that allows for deposition of catalyst NPs over large areas with controlled surface coverage that is compatible with roll-to-roll processing.

Solution deposition of thin layers of precursors, such as metal acetates, for forming catalytic NPs has also been used to grow carbon nanotubes[32−35] but does not allow independent control of the NP size and density of coverage. The catalyst NPs used here (d > 100 nm) are also much larger than those used for single-walled carbon nanotubes that are commonly obtained from metal acetates.[33] Microcontact printing has also been used to pattern catalyst NPs[36,37] or precursors for catalyst NPs[38,39] for the growth of carbon nanotubes, but airbrushing is potentially faster for applications that do not require periodic arrays, for example, for coating windows or buildings with VACNFs.

Deposition of catalyst NPs and subsequent growth of VACNFs have been conducted primarily on Si(111) substrates, but some other substrates including Mo, Nb, W, and Cr have

Received: May 19, 2013
Accepted: August 19, 2013
Published: September 9, 2013

   dx.doi.org/10.1021/am401889t | ACS Appl. Mater. Interfaces 2013, 5, 8955−8960

also been explored.[40,41] Si has limited ability to withstand harsh processing conditions compared to most metals, making it an unsuitable choice for use as a substrate for VACNF growth for some applications.[29] Moreover, most of the applications listed above require conductive pathways between the VACNFs and a metal substrate that is connected to an electrical circuit. Si substrates provide a beneficial Si-enriched coating on the VACNFs that enhances their mechanical properties, but growth of VACNFs with Si-enriched coatings on other substrates requires an additional source of Si.[42] Hereafter, we refer to these Si-enriched coatings simply as Si coatings, with the understanding that they may also contain C, N, and O.

Here, we report airbrushing of Ni NPs onto Si, Al, Cu, and Ti substrates, followed by VACNF growth via PECVD. The distribution and surface density of the VACNFs are defined by the pattern of the Ni NPs obtained through airbrushing because the Ni NPs catalyze VACNF growth. Detailed structural and compositional analyses reveal the effects of interactions between the catalyst NPs and metal substrates and prove the existence of Si coatings on the VACNFs.

EXPERIMENTAL SECTION

NP Synthesis. 1-Octadecene (5.0 mL, 90%, Sigma-Aldrich), oleylamine (5.0 mL, 80−90% C_{18} content, Acros), and Ni(II) acetylacetonate hydrate (0.50 g, 98%, TCI America) were mixed and allowed to degas under vacuum for 2 h at 60−80 °C. The solution was then backfilled with nitrogen and heated at a rate of 10 °C/min to 230 °C and held at this temperature for 30 min. After completing the reaction, the NPs were flocculated by adding ethanol, followed by centrifugation for purification. The supernatant was discarded, and the NPs were redispersed into different nonpolar solvents (pentane, hexanes, or heptane).

NP Airbrushing onto Substrates. Varying concentrations of Ni NPs were deposited onto ∼1 cm^2 Si wafers and Al Alloy 6061, Cu Alloy 101, and Ti grade 2 foils (obtained from McMaster Carr) using an Iwata Eclipse HP-CS airbrush. For specifying the concentration, Ni NP solutions with an optical absorbance of 1 at 600 nm were denoted as 1× concentration. The airbrush was operated with compressed air at 50 psi. Prior to airbrushing, the metal foils were cleaned by sonicating in acetone, rinsing with methanol, and then allowing the residual solvent to dry. The NPs were airbrushed onto the substrates in two short pulses of 0.5 s each, with the tip of the nozzle held 0.3 m from the substrate. There was a brief pause between pulses to ensure that the solvent had completely evaporated. For the metal foils, two 0.5 s pulses of a dispersion of 0.5 g of Si micropowder (Atlantic Equipment Engineers, SI-100, Technical Grade Silicon Metal Powder) in 10 mL of acetone were airbrushed over the same area. The duration of spraying and the distance from the airbrush nozzle to the substrate were the same for all samples.

VACNF Growth. VACNFs were grown on the substrates with airbrushed catalytic NPs (and Si micropowder for the metal substrates) by direct-current glow discharge PECVD. The substrates were heated to 600 °C under a 0.05 Torr vacuum, and then the chamber was backfilled with 4 Torr ammonia. Acetylene (45 sccm) and ammonia (85 sccm) were used as the carbon source and etchant gases, respectively. The sample was grown for 2 h at a current of 0.5 A, temperature of 600 °C, and pressure of 4 Torr. The chamber was evacuated following growth, and the substrate was allowed to cool to room temperature under vacuum.

Characterization. Conventional transmission electron microscopy (TEM) images were acquired on a JEOL 2000FX microscope operated at 200 kV, and scanning electron microscopy (SEM) was performed on a Zeiss Merlin field emission SEM. High-angle annular dark-field scanning TEM (HAADF-STEM) and bright-field (BF) STEM images, and energy dispersive X-ray spectroscopy (EDS) maps were acquired with a probe-corrected FEI Titan G2 60-300 S/TEM operated at 200 kV and equipped with a Super-X EDS detector system. The elemental EDS data were acquired for 8 min with a beam current of ∼80 pA, and maps were formed using the K_α X-ray signal of the corresponding element. Histograms of the VACNF diameters for each substrate were obtained by counting SEM measurements of 200 VACNFs from each substrate.

RESULTS AND DISCUSSION

Growth of VACNFs from Sparse Coverage of Airbrushed Ni NPs. To characterize the airbrushing process, VACNFs were first grown on pieces of a Si wafer using Ni NPs deposited by airbrushing. The Ni NPs (Figure 1a) were synthesized according to a modification of a previously reported method,[43] resulting in dendritic shapes and an average diameter of d_{NP} = 186 nm. The spatial distributions of the Ni NPs deposited through airbrushing onto Si(111) substrates from several solvents at different concentrations and of the Si-coated VACNFs grown from these Ni NPs are shown in Figure 1b−i. Alkanes were chosen as solvents, where the evaporation rate decreases as the chain length increases, to observe how the drying kinetics affected the deposited structures. The Ni NPs dispersed well into pentane and hexanes at the 1× concentration, but significant clustering was observed after deposition onto the Si substrate (Figure 1b,c). The NPs were more uniformly distributed on the Si substrate when airbrushed from a heptane suspension, for which three different concentrations of the airbrushing solution (0.25×, 0.5× and 1×) were used (Figure 1d,f,h). Two important observations from images of VACNFs grown from these NPs (Figure 1e,g,i and Supporting Information, Figure S1) are the following: (1) The density of VACNFs is proportional to the concentration of the Ni NPs in the airbrushing solution. Greater concentrations of NPs give more densely packed VACNFs. (2) Despite minor clustering of the Ni NPs prior to VACNF growth, there is less clustering in the distribution of the VACNFs. This suggests that the Ni NPs become somewhat mobile during the pregrowth phase prior to the start of VACNF growth, when the NPs become pinned at the tips of the VACNFs. In contrast to our recent study, where we showed that trioctylphosphine (TOP) ligands coating ∼25 nm diameter Ni NPs are converted into graphitic shells that protect the NPs from agglomerating during the pregrowth stage,[43] some of the NPs reported here become mobile, but the Ni cores do not coalesce together. The NPs used in this study were synthesized without using any TOP, and oleylamine is a more weakly binding ligand than TOP that appears to reduce the NP mobility but does not completely pin them in their as-deposited state. The clustering seen here is not as severe or as problematic as the agglomeration of metal catalyst NPs in thin film lithography deposition approaches, however, where NP singularity is achieved via sufficient separation of patterned islands, and undesired NP mobility remains a significant challenge.[44]

VACNF Deposition and Growth on Al, Ti, and Cu Foils. Ni NPs were airbrushed onto Al Alloy 6061, Ti grade 2, and Cu Alloy 101 foils. Heptane was selected as the solvent for airbrushing because it gave more uniform deposition than pentane and hexanes. Prior to VACNF growth, Si micropowder was separately airbrushed onto the substrate, which was required to serve as a Si source for depositing Si coatings onto the surfaces of the VACNFs that provide important structural support[42] and impart sufficient rigidity for the nanofibers to point straight out of the plane of the substrate. Si coatings on VACNFs have facilitated further processing and applications, such as the deposition of polymer coatings onto

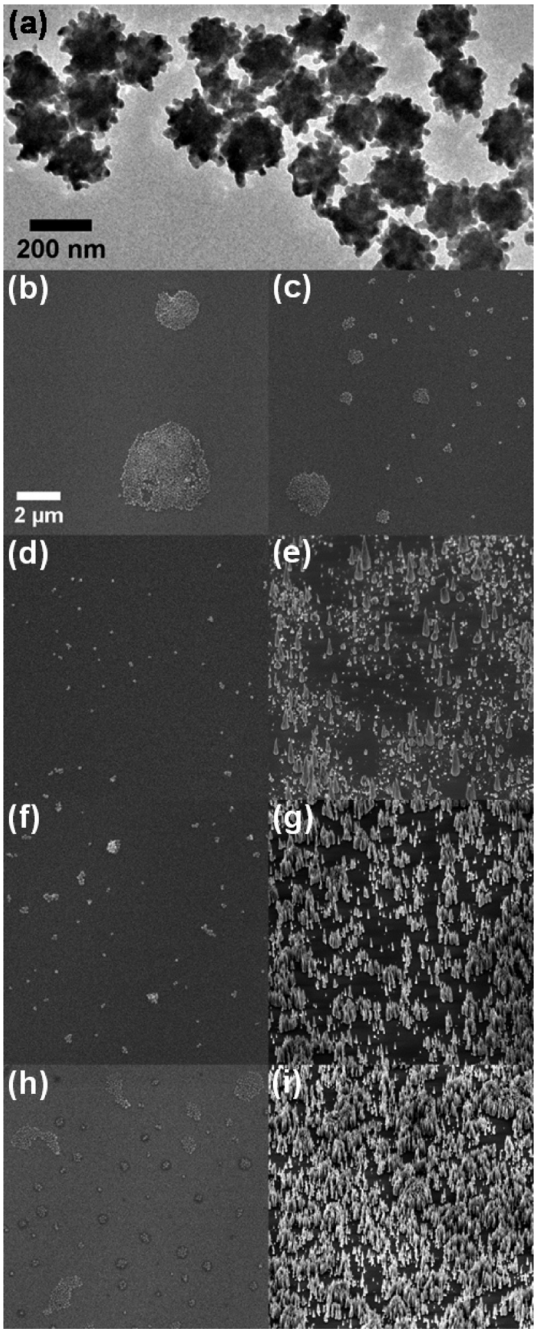

Figure 1. (a) TEM image of Ni NPs and (b–i) SEM images of airbrushed Ni NPs and VACNFs on Si substrates with a common scale bar: (b,c) 1× Ni NPs dispersed in pentane and hexanes, respectively, (d,f,h) Ni NPs in heptane with respective concentrations of 0.25×, 0.5×, and 1×, and (e,g,i) VACNFs grown from the corresponding samples in (d,f,h).

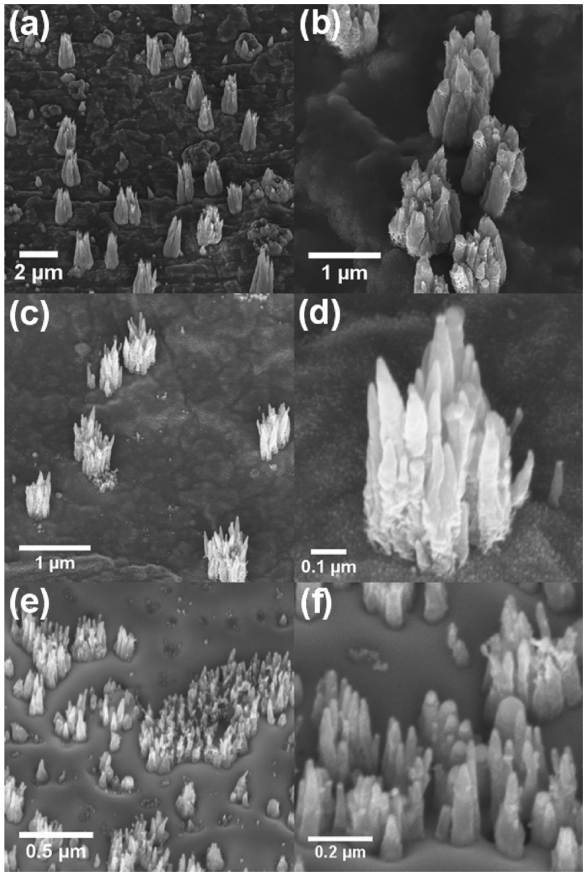

Figure 2. SEM images of VACNFs grown on metal foils of (a,b) Al Alloy 6061, (c,d) Ti grade 2, and (e,f) Cu Alloy 101.

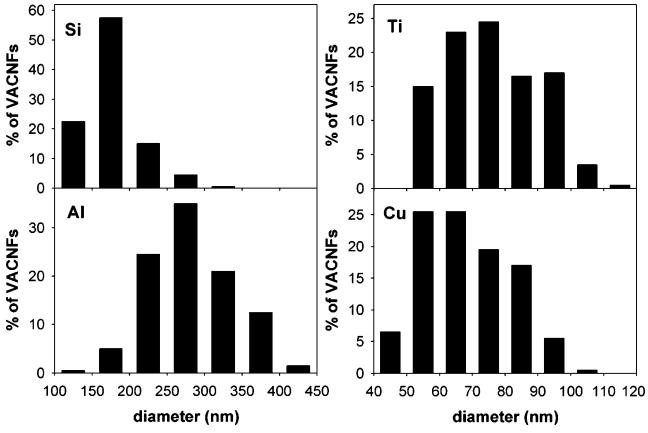

Figure 3. Histograms of VACNF diameters measured by SEM for VACNFs grown on Si wafers and Al, Ti, and Cu foils.

arrays of VACNFs without the fibers collapsing and allowing VACNFs to be pressed into and to penetrate brain tissue multiple times without mechanical degradation of the fibers.[8,12] The basal diameters (averages given in parentheses) of the VACNFs on the Al (230 nm), Ti (80 nm), and Cu (45 nm) foils were measured manually from SEM images (Figure 2) and tabulated in histograms (Figure 3). Typical fiber heights were ~0.1–2.0 μm. The VACNFs are conical in shape because sidewall deposition of C accompanies catalytic growth.[42] More C accumulates at the bases of the VACNFs because they were the first parts formed and experience the longest time for sidewall deposition, resulting in a conical shape.[45] The fact that the VACNFs are vertically aligned when grown on substrates other than Si but in the presence of airbrushed Si micropowder confirms that the micropowder serves as the Si source for the Si coatings.

Si-Enriched Coating. Here, the primary focus is on characterizing the Si-coating on the VACNFs because their internal structure is already known from previous studies.[46] STEM images and energy-dispersive X-ray spectroscopy (EDS) maps for VACNFs grown on Al and Cu foils are presented in

dx.doi.org/10.1021/am401889t | ACS Appl. Mater. Interfaces 2013, 5, 8955–8960

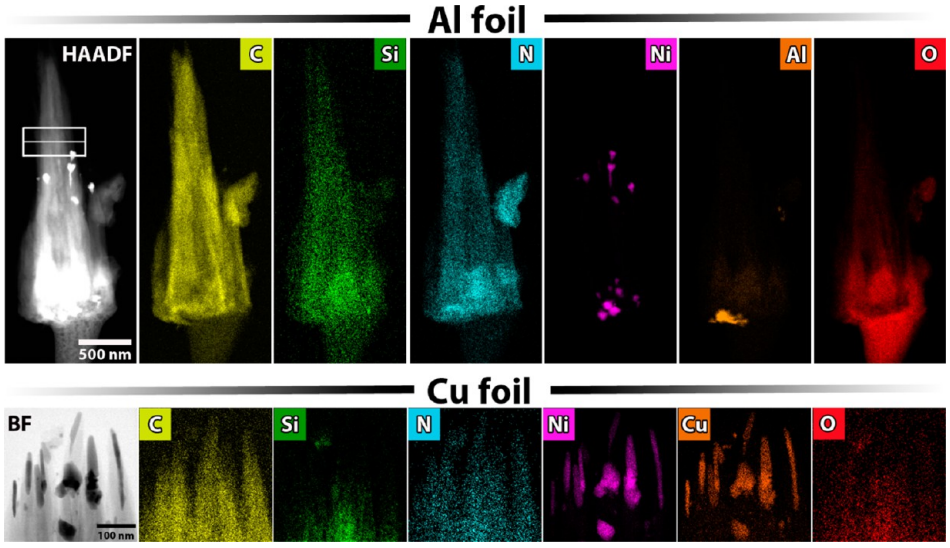

Figure 4. HAADF-STEM/BF-STEM and elemental mapping by EDS of VACNFs grown on Al and Cu substrates. White box inset in the HAADF-STEM image for growth on Al indicates the region of the EDS line profiles in Figure 5.

Figure 4. An additional HAADF-STEM image for the VACNFs grown on Cu is provided in the Supporting Information, Figure S2. The Si signal is the most intense in the base of the fibers, which is consistent with sidewall deposition of Si and the longer exposure time of the base to the reactive plasma environment. N is also present throughout the fibers, which is incorporated from the ammonia etchant gas. An EDS line profile (Figure 5)

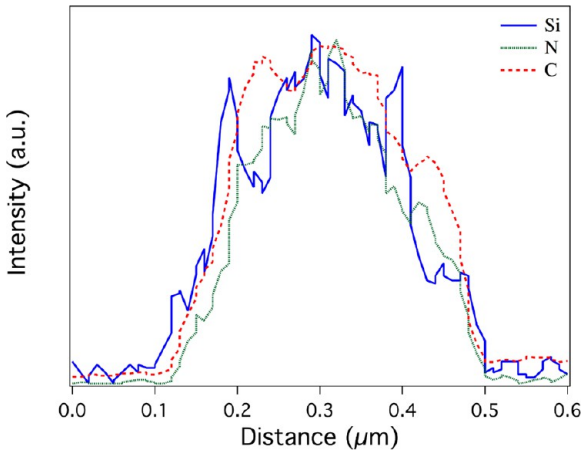

Figure 5. EDS line profiles for Si, N, and C acquired toward the top of a VACNF grown on Al, where the region of the line profiles is indicated on the HAADF-STEM panel in Figure 4. Boxcar averaging was performed to smooth each data set. Each plot has been normalized to its maximum value.

across the diameter of a fiber shows two prominent peaks in the Si signal on the sides of the fiber, which is consistent with a Si-enriched coating that may also contain C, N, and O. The amount of these species other than Si in the coating is unclear, but the Si powder is required as a Si source for growth on metal foils. While the VACNF growth temperature is well below the bulk meting point of Si, the plasma in PECVD may drive volatilization of Si, and the highly reactive environment may also cause surface reactions resulting in gaseous Si-containing molecular species. The reactive Si species are then deposited on the sidewalls of the VACNFs.

NP–Substrate Interactions. The nature of the catalyst NPs and the substrate together determine the structure of the nanofibers. Even though much research has been conducted to produce VACNFs with uniform spatial distributions on Si wafers, the interaction of catalyst NPs with metal substrates at elevated temperatures prior to nanofiber growth remains a significant challenge. Two possible kinds of NP-metal foil interactions that are consistent with our results are the following: (1) There may be interdiffusion between the catalyst NPs and the metal substrate, which is expected for Cu, since CuNi alloys are the classic example of binary isomorphous systems. EDS mapping (Figure 4) confirms that Cu diffuses into the catalytic NPs that are suspended at the tips of the VACNFs. In some cases, ligands coating the NPs might also impede the alloying process. (2) Changing the metal selected for the substrate can alter the NP-substrate interaction. In the case of Si, the average basal VACNF diameter (151 nm) matches d_{NP} (186 nm) well. For Al substrates, the broad distribution of VACNF diameters that generally exceeds d_{NP} indicates agglomeration of the catalyst NPs prior to VACNF growth. The average VACNF basal diameters on Ti and Cu substrates are significantly smaller than d_{NP}, which suggests that the metal substrate in some cases may facilitate division of the catalyst NPs into smaller NPs. Growth of VACNFs directly onto Cu substrates overcomes a challenge in the fabrication of Li-ion batteries, where it is desirable to anchor carbon nanostructures that serve as anodes to Cu film current collectors for connecting the batteries to an external circuit.[47,48] Carbon nanostructures bound to Cu substrates are also of interest as thermal interface materials.[49−51]

CONCLUSIONS

In summary, airbrushing is a simple and economical technique for depositing catalyst NPs for growth of VACNFs over large areas that could also be applied to the growth of carbon nanotubes and inorganic nanowires. Unlike lithographic approaches for preparing catalyst NPs, airbrushing does not require a flat substrate. We have demonstrated VACNF growth on several metal substrates, where addition of Si micropowder allows the growth of Si-enriched coatings that make the VACNFs mechanically rigid. Use of ligand-stabilized NPs also

inhibits coalescence of the NP cores, which helps to preserve a narrow distribution of VACNF diameters. For growth on different kinds of metal foils, the interaction of the catalyst NP with the metal foil determines the VACNF diameter and whether interdiffusion between the NP and foil occurs. Growth of VACNFs directly onto Cu substrates overcomes a significant technological challenge that will facilitate the use of VACNFs in Li-ion batteries and thermal interface materials.

■ ASSOCIATED CONTENT

Supporting Information

Top-view SEM images of VACNFs grown from Ni NPs airbrushed from heptane and HAADF-STEM image of VACNFs grown on Cu foil. This material is available free of charge via the Internet at http://pubs.acs.org.

■ AUTHOR INFORMATION

Corresponding Author

*E-mail: jbtracy@ncsu.edu.

Notes

The authors declare no competing financial interest.

■ ACKNOWLEDGMENTS

This research was supported by the National Science Foundation Grant DMR-1056653 (to J.B.T.) and the Department of the Defense, Defense Threat Reduction Agency (to A.V.M). A portion of this research was conducted at the Center for Nanophase Materials Sciences, which is sponsored at Oak Ridge National Laboratory by the Scientific User Facilities Division, Office of Basic Energy Sciences, U.S. Department of Energy. The content of the information herein does not necessarily reflect the position or the policy of the Federal Government, and no official endorsement should be inferred. M.F.S. acknowledges support from a Republic of Turkey, Ministry of National Education fellowship. We thank Timothy E. McKnight for helpful discussions. This work made use of the Analytical Instrumentation Facility at NCSU.

■ REFERENCES

(1) Ye, Q.; Cassell, A. M.; Liu, H. B.; Chao, K. J.; Han, J.; Meyyappan, M. *Nano Lett.* **2004**, *4*, 1301−1308.
(2) McKnight, T. E.; Melechko, A. V.; Griffin, G. D.; Guillorn, M. A.; Merkulov, V. I.; Serna, F.; Hensley, D. K.; Doktycz, M. J.; Lowndes, D. H.; Simpson, M. L. *Nanotechnology* **2003**, *14*, 551−556.
(3) Guillorn, M. A.; McKnight, T. E.; Melechko, A.; Merkulov, V. I.; Britt, P. F.; Austin, D. W.; Lowndes, D. H.; Simpson, M. L. *J. Appl. Phys.* **2002**, *91*, 3824−3828.
(4) McKnight, T. E.; Melechko, A. V.; Hensley, D. K.; Mann, D. G. J.; Griffin, G. D.; Simpson, M. L. *Nano Lett.* **2004**, *4*, 1213−1219.
(5) Pantarotto, D.; Singh, R.; McCarthy, D.; Erhardt, M.; Briand, J. P.; Prato, M.; Kostarelos, K.; Bianco, A. *Angew. Chem., Int. Ed.* **2004**, *43*, 5242−5246.
(6) Mann, D. G. J.; McKnight, T. E.; Melechko, A. V.; Simpson, M. L.; Sayler, G. S. *Biotechnol. Bioeng.* **2007**, *97*, 680−688.
(7) Mann, D. G. J.; McKnight, T. E.; McPherson, J. T.; Hoyt, P. R.; Melechko, A. V.; Simpson, M. L.; Sayler, G. S. *ACS Nano* **2008**, *2*, 69−76.
(8) Pearce, R. C.; Railsback, J. G.; Anderson, B. D.; Sarac, M. F.; McKnight, T. E.; Tracy, J. B.; Melechko, A. V. *ACS Appl. Mater. Interfaces* **2013**, *5*, 878−882.
(9) Fletcher, B. L.; Retterer, S. T.; McKnight, T. E.; Melechko, A. V.; Fowlkes, J. D.; Simpson, M. L.; Doktycz, M. J. *ACS Nano* **2008**, *2*, 247−254.
(10) Nguyen-Vu, T. D. B.; Chen, H.; Cassell, A. M.; Andrews, R. J.; Meyyappan, M.; Li, J. *IEEE Trans. Biomed. Eng.* **2007**, *54*, 1121−1128.
(11) Andrews, R. J. *J. Nanosci. Nanotechnol.* **2009**, *9*, 5008−5013.
(12) Yu, Z.; McKnight, T. E.; Ericson, M. N.; Melechko, A. V.; Simpson, M. L.; Morrison, B., III *Nano Lett.* **2007**, *7*, 2188−2195.
(13) Han, W. Q.; Zettl, A. *Nano Lett.* **2003**, *3*, 681−683.
(14) Cassell, A. M.; Li, J.; Nguyen-Vu, T.-D. B.; Koehne, J. E.; Chen, H.; Andrews, R.; Meyyappan, M. *J. Nanosci. Nanotechnol.* **2009**, *9*, 5038−5046.
(15) Koehne, J. E.; Marsh, M.; Boakye, A.; Douglas, B.; Kim, I. Y.; Chang, S.-Y.; Jang, D.-P.; Bennet, K. E.; Kimble, C.; Andrews, R.; Meyyappan, M.; Lee, K. H. *Analyst* **2011**, *136*, 1802−1805.
(16) Chhowalla, M.; Teo, K. B. K.; Ducati, C.; Rupesinghe, N. L.; Amaratunga, G. A. J.; Ferrari, A. C.; Roy, D.; Robertson, J.; Milne, W. I. *J. Appl. Phys.* **2001**, *90*, 5308−5317.
(17) Semet, V.; Binh, V. T.; Vincent, P.; Guillot, D.; Teo, K. B. K.; Chhowalla, M.; Amaratunga, G. A. J.; Milne, W. I.; Legagneux, P.; Pribat, D. *Appl. Phys. Lett.* **2002**, *81*, 343−345.
(18) Chhowalla, M.; Ducati, C.; Rupesinghe, N. L.; Teo, K. B. K.; Amaratunga, G. A. J. *Appl. Phys. Lett.* **2001**, *79*, 2079−2081.
(19) AuBuchon, J. F.; Chen, L. H.; Gapin, A. I.; Jin, S. H. *Chem. Vap. Deposition* **2006**, *12*, 370−374.
(20) Guillorn, M. A.; Yang, X.; Melechko, A. V.; Hensley, D. K.; Hale, M. D.; Merkulov, V. I.; Simpson, M. L.; Baylor, L. R.; Gardner, W. L.; Lowndes, D. H. *J. Vac. Sci. Technol., B* **2004**, *22*, 35−39.
(21) Tse, K.-Y.; Zhang, L.; Baker, S. E.; Nichols, B. M.; West, R.; Hamers, R. J. *Chem. Mater.* **2007**, *19*, 5734−5741.
(22) Liu, J.; Essner, J.; Li, J. *Chem. Mater.* **2010**, *22*, 5022−5030.
(23) Metz, K. M.; Tse, K.-Y.; Baker, S. E.; Landis, E. C.; Hamers, R. J. *Chem. Mater.* **2006**, *18*, 5398−5400.
(24) Metz, K. M.; Goel, D.; Hamers, R. J. *J. Phys. Chem. C* **2007**, *111*, 7260−7265.
(25) Metz, K. M.; Colavita, P. E.; Tse, K.-Y.; Hamers, R. J. *J. Power Sources* **2012**, *198*, 393−401.
(26) Zhang, C.; Hu, J.; Wang, X.; Zhang, X.; Toyoda, H.; Nagatsu, M.; Meng, Y. *Carbon* **2012**, *50*, 3731−3738.
(27) Retterer, S. T.; Melechko, A.; Hensley, D. K.; Simpson, M. L.; Doktycz, M. J. *Carbon* **2008**, *46*, 1378−1383.
(28) Fowlkes, J. D.; Melechko, A. V.; Klein, K. L.; Rack, P. D.; Smith, D. A.; Hensley, D. K.; Doktycz, M. J.; Simpson, M. L. *Carbon* **2006**, *44*, 1503−1510.
(29) Melechko, A. V.; Merkulov, V. I.; McKnight, T. E.; Guillorn, M. A.; Klein, K. L.; Lowndes, D. H.; Simpson, M. L. *J. Appl. Phys.* **2005**, *97*, 041301.
(30) Akhavan, V. A.; Goodfellow, B. W.; Panthani, M. G.; Reid, D. K.; Hellebusch, D. J.; Adachi, T.; Korgel, B. A. *Energy Environ. Sci.* **2010**, *3*, 1600−1606.
(31) Zhu, Y.; Lu, W.; Sun, Z.; Kosynkin, D. V.; Yao, J.; Tour, J. M. *Chem. Mater.* **2011**, *23*, 935−939.
(32) Mukhopadhyay, K.; Koshio, A.; Tanaka, N.; Shinohara, H. *Jpn. J. Appl. Phys.* **1998**, *37*, L1257.
(33) Hu, M.; Murakami, Y.; Ogura, M.; Maruyama, S.; Okubo, T. *J. Catal.* **2004**, *225*, 230−239.
(34) Murakami, Y.; Yamakita, S.; Okubo, T.; Maruyama, S. *Chem. Phys. Lett.* **2003**, *375*, 393−398.
(35) Mukhopadhyay, K.; Koshio, A.; Sugai, T.; Tanaka, N.; Shinohara, H.; Konya, Z.; Nagy, J. B. *Chem. Phys. Lett.* **1999**, *303*, 117−124.
(36) Ding, L.; Li, C.; Zhou, W.; Chu, H.; Sun, X.; Cao, Z.; Yang, Z.; Yan, C.; Li, Y. *Eur. J. Inorg. Chem.* **2010**, *2010*, 4357−4362.
(37) Jie, Y.; Niskala, J. R.; Johnston-Peck, A. C.; Krommenhoek, P. J.; Tracy, J. B.; Fan, H.; You, W. *J. Mater. Chem.* **2012**, *22*, 1962−1968.
(38) Zhou, W.; Rutherglen, C.; Burke, P. *Nano Res.* **2008**, *1*, 158−165.
(39) Xu, P.; Ji, X.; Qi, J.; Yang, H.; Zheng, W.; Abetz, V.; Jiang, S.; Shen, J. *J. Nanosci. Nanotechnol.* **2010**, *10*, 508−513.
(40) Kabir, M. S.; Morjan, R. E.; Nerushev, O. A.; Lundgren, P.; Bengtsson, S.; Enoksson, P.; Campbell, E. E. B. *Nanotechnology* **2006**, *17*, 790.

(41) Pearce, R. C.; Vasenkov, A. V.; Hensley, D. K.; Simpson, M. L.; McKnight, T. E.; Melechko, A. V. *ACS Appl. Mater. Interfaces* **2011**, *3*, 3501−3507.
(42) Melechko, A. V.; McKnight, T. E.; Hensley, D. K.; Guillorn, M. A.; Borisevich, A. Y.; Merkulov, V. I.; Lowndes, D. H.; Simpson, M. L. *Nanotechnology* **2003**, *14*, 1029−1035.
(43) Wang, J.; Johnston-Peck, A. C.; Tracy, J. B. *Chem. Mater.* **2009**, *21*, 4462−4467.
(44) Melechko, A. V.; Pearce, R. C.; Hensley, D. K.; Simpson, M. L.; McKnight, T. E. *J. Phys. D: Appl. Phys.* **2011**, *44*, 174008.
(45) Merkulov, V. I.; Guillorn, M. A.; Lowndes, D. H.; Simpson, M. L.; Voelkl, E. *Appl. Phys. Lett.* **2001**, *79*, 1178−1180.
(46) Melechko, A. V.; Klein, K. L.; Fowlkes, J. D.; Hensley, D. K.; Merkulov, I. A.; McKnight, T. E.; Rack, P. D.; Horton, J. A.; Simpson, M. L. *J. Appl. Phys.* **2007**, *102*, 074314.
(47) Venkatachalam, S.; Zhu, H. W.; Masarapu, C.; Hung, K. H.; Liu, Z.; Suenaga, K.; Wei, B. Q. *ACS Nano* **2009**, *3*, 2177−2184.
(48) Lahiri, I.; Oh, S.-M.; Hwang, J. Y.; Kang, C.; Choi, M.; Jeon, H.; Banerjee, R.; Sun, Y.-K.; Choi, W. *J. Mater. Chem.* **2011**, *21*, 13621−13626.
(49) Huang, H.; Liu, C. H.; Wu, Y.; Fan, S. *Adv. Mater.* **2005**, *17*, 1652−1656.
(50) Kordas, K.; Toth, G.; Moilanen, P.; Kumpumaki, M.; Vahakangas, J.; Uusimaki, A.; Vajtai, R.; Ajayan, P. M. *Appl. Phys. Lett.* **2007**, *90*, 123105.
(51) Lin, W. O., R.V.; Liang, Q.; Zhang, R.; Kyoung-Sik Moon; Wong, C. P. Vertically Aligned Carbon Nanotubes on Copper Substrates for Applications as Thermal Interface Materials: From Synthesis to Assembly. In *Proceedings of the 59th IEEE Electronic Components and Technology Conference*, San Diego, CA, May 26−29, 2009; pp 441−447.